

## Occurrence of recent dedolomite crust on pedogenic calcrete in Al-Jabal Al-Akhdar, Northern Oman

Fikry Khalaf\*, Abdullah Al-Zamel

*Dept. of Earth and Environmental Sciences, Faculty of Science, Kuwait University, Kuwait*

*\*Fikry\_khalaf@hotmail.com*

### Abstract

Rusty dedolomitized crust occurs in fractured pedogenic calcrete horizon within terra rossa soil contained in shallow phytokarstic cavities in the calcareous rocks exposed at Al-Jabal Al-Akhdar Mountain, Oman. Two lithotypes were recognized: (a) dedolomitized detrital dolomite and (b) dedolomitized authigenic dolomite. The first is light brownish, has an undulating sharp contact with the nodular calcretes and consists of euhedral to subhedral moderately to poorly sorted dolomite grains floating in a micritic groundmass. The second is relatively thicker, dark brown, and consists of idiopathic mosaic of moderately sorted well euhedral dolomite crystals that reach up to 200  $\mu\text{m}$  in size. Microscopic examination of stained thin sections indicated that most of both detrital and authigenic dolomite crusts have been partially or completely dedolomitized. XRD analysis indicated that both types of crusts mostly consist of calcite and dolomite with traces of quartz, where abundance of calcite reflects their dedolomitization. The chemical composition of these crusts reflects their mineralogy. The paragenetic events of the crust formation are discussed. The availability of dolomitic source rocks and the present prevailed semi-arid climate characterized by intermittent wet and dry periods have played a significant role in its development. This work presents a unique mode of occurrence of dedolomitized dolomite associated with recent pedogenic calcretes.

**Keywords:** Al-Jabal Al-Akhdar; calcrete; crust; dedolomite; Oman.

### 1. Introduction

Dedolomite is a term introduced by Von Morlot (1847) for dolomite replaced by calcite via interaction with high Ca/Mg ratios fluids. Dedolomitisation is typically associated with near-surface conditions (Chilingar, 1956; Goldberg, 1967; Holail *et al.*, 1988; Kenny, 1992; Khalaf & Abdal, 1993; Cantrell *et al.*, 2007; Rameil, 2008; Nader *et al.*, 2008). Several authors have proposed that dedolomitisation is facilitated by the presence of sulfate-rich brines during burial diagenesis (Katz, 1968; Carpenter *et al.*, 1974; Kharaka *et al.*, 1977; Land & Prezbindowski, 1981; Budai *et al.*, 1984). Dedolomite occurrences without evidence of evaporites have also been reported (Chafetz, 1972; Stoessel *et al.*, 1987; Theriault & Hutcheon, 1987). De Groot (1967) found that effective dedolomitisation requires: (1) a high fluid flow rate to remove Mg and keep the Ca/Mg ratio elevated, (2) a low CO<sub>2</sub> partial pressure, similar to that of the atmosphere, and (3) a temperature below 50°C. Dedolomitisation is generally achieved through a one-step process in which dolomite dissolution and calcite precipitation are simultaneous (Evamy, 1967; Al-Hashimi & Hemingway, 1973; Back *et al.*, 1983; Khalaf & Abdal, 1993). However, some authors have suggested the occurrence of a two-step process involving the dissolution of dolomite and formation of cavities, and later precipitation of calcite from the same solution (Warrak, 1974; Kenny, 1992) or from a different solution at a different

time (Jones *et al.*, 1989; James *et al.*, 1993). Coniglio (2003) reported that dedolomitization process includes both neomorphic replacement of dolomite by calcite and dolomite dissolution followed by calcite cementation.

Dedolomitisation also has economic significance; it can alter the porosity and permeability of carbonates, and thus affect reservoir quality (Escorcia *et al.*, 2013).

The presence of dolomite associated with calcretes has been recorded by many authors (Watts, 1980; Hutton & Dixon, 1981; Phillips & Milnes, 1988; Dixon, 2010). The origin of this dolomite has simply been attributed to an increase in the Mg/Ca ratio of downward-percolating soil solutions associated with calcite precipitation higher in the soil profile (Hutton & Dixon, 1981; Khalaf, 1990; Dixon, 2010). Most reported dolocrete, or dolomitised calcrete, occurs in profiles that reflect various grades of dolocretisation within soil or clastic sediments (Netterberg, 1980). Dedolomitised dolomite crusts associated with calcrete have rarely been described in the literature.

A well-exposed, thick sequence of shallow-marine dolomitised limestones in the Jabal Akhdar Mountains, northern Oman is characterised by the abundant occurrence of relatively thin phytokarst pockets filled with calcretised terra rossa soil (Khalaf & Al Zamel, 2016).

The main objective of present paper is to provide for the first time information on the mode of occurrence of dedolomite crust that coats fractured recent pedogenic nodular calcrete deposits within a terra rossa soil. It also discusses its textures, mineralogy and genesis.

## 2. General setting

The study area is located approximately 2000 m above sea level in the Jabal Akhdar Mountains, northern Oman (Figure 1). In this region, a 2.5-km-thick dolomitised limestone succession known as the Hajar Supergroup is exposed. From bottom to top, this succession includes Permian limestone (Saiq Formation); Triassic dolostone (Mahil Formation); Jurassic limestone, dolostone and siliciclastic red beds (Sahtan Group); and lower Cretaceous–Cenomanian limestone (Kahmah and Wasia Groups) (Saddiqi *et al.*, 2006; Koehrer *et al.*, 2010; Baud & Richoz, 2013).

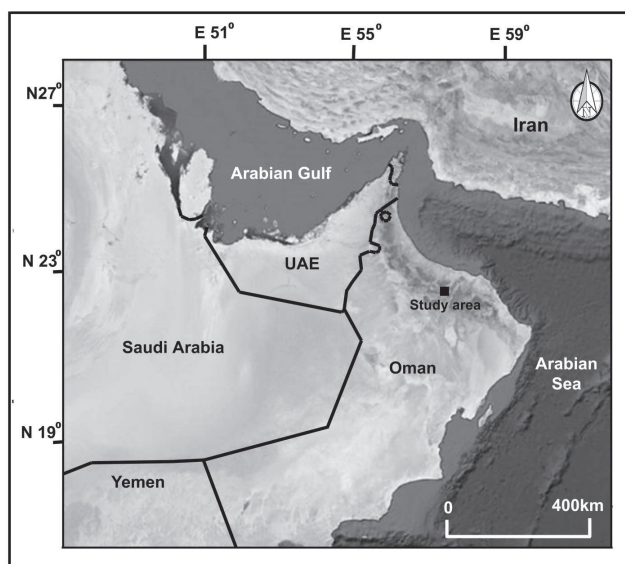


**Figure 1.** Location map of the study area.

The Sultanate of Oman lies in an arid to semi-arid global climatic zone characterised by a subtropical dry, hot, desert climate with low annual rainfall. However, unlike the climate of the surrounding desert area, that of the Al-Jabal Al-Akhdar region tends to be more similar to that of the Mediterranean zone. In general, annual rainfall in this region ranges from 115 to 413 mm. Winter temperatures range between 1 and 21.5°C, but temperatures tend to be hot in summer, with an annual average between 31°C and 34°C and exceeding 35°C in some years. The average humidity ranges between 22% and 55%, in summer and winter, respectively (Al-Busaidi, 2012).

## 3. Field occurrence

Small, shallow cavities commonly occur at the contact between the extensively cracked Mahil dolomitized limestone and the hard blackish carbonates of the Saiq Formation. Some of these cavities are exposed along a road cut in the Daen Al Hamra area (23°7'22.02 N and 57°35'50.07 E). These cavities may have formed through localized dissolution of the calcareous bedrock along vertical fractures during the Holocene wet period. They reach more than 3 m in thickness and extend laterally for more than 5 m. However, they are highly variable in size and morphology.

Khalaf & Al-Zamel (2016) studied a Holocene calcrete deposit associated with the terra rossa soil that fills these cavities. They found that the calcrete deposit mostly occurs as clustered nodules and as discrete rhizcretions associated with tree roots within the terra rossa soil. Based on detailed petrographic, mineralogical and geochemical investigation, they concluded that this calcrete is pedogenic and has been precipitated from freshwater within a shallow terra rossa soil thriving with microorganisms that form thrombolitic calcareous microbialites. They further suggested that this calcrete developed during the prolonged durations of alternating wet and dry periods that characterize the present climatic conditions of the Al-Jabal Al-Akhdar region.

An excavated ditch within one of these calcrete fill cavities exposes a massive whitish calcrete deposit similar to that described by Khalaf & Al-Zamel (2016). It is approximately 6 m thick and of limited lateral extent. This calcrete deposit is almost entirely covered by a rusty crust. Its surface displays features similar to those of flowstone. Close inspection of at this crust reveals that it varies in thickness between several millimetres to 10 cm and consists of two layers: a hard, dark brown layer that commonly overlies a relatively soft, light brown layer (Figure 2A). Occasionally, the hard, dark brown layer directly covers the main calcrete mass (Figure 2C). It varies in thickness, with a maximum observed thickness of approximately 6 cm. It is characterized by a smooth, crenulated surface with abundant mammillary features and dissolution cavities. The latter are commonly bounded by hard veins about 2 cm thick (Figure 2B). The soft, light brown layer of the crust commonly coats the main calcretic mass with a diffused contact. It is generally friable, varies in thickness and may reach up to 5 cm in thickness at some locations.

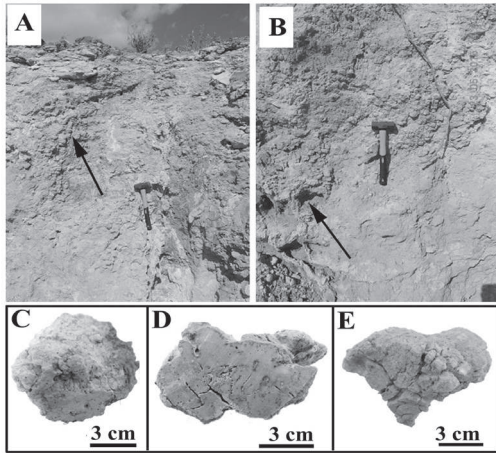


**Figure 2.** (A) and (B) Field photographs of the dedolomitised crust. Arrow in (A) points to a mammillary feature; arrow in (B) points to a dissolution cavity; (C) brownish crust coating a pedogenic calcrete nodule; (D) slab of crust sample showing open desiccation cracks and abundant iron-oxide spots; (E) crust sample showing wide open desiccation cracks.

#### 4. Methodology

The field occurrence and surface features of the crust were described, and representative samples were collected. Nine samples were collected of the light brown crust, and six of the hard, dark brown crust. Rock slabs from all crust samples were finely polished and described. Two thin sections were prepared from each sample, and one of each pair was stained with Alizarin Red S to distinguish calcite and dolomite (Dickson, 1966). Thin sections were investigated using a research polarising microscope with an attached digital camera.

The main mineral constituents of all collected samples were identified using a BrukerD5000 X-ray diffractometer (XRD). The XRD patterns were collected in a  $2\theta$  angular range between  $10^\circ$  and  $80^\circ$ , with a  $2\theta$  scan step of  $0.015^\circ$  and a step time of 2 s, using  $\text{CuK}\alpha 1$  radiation ( $\lambda = 1.5406 \text{ \AA}$ ) and a Ni filter at a voltage of 40 kV and a current of 40 mA. The computer program DIFFRACplus, with the International Centre for Diffraction Data (ICDD) library, was used for mineral identification and semi-quantification. Semi-quantitative analysis of the major oxides within the studied samples was carried out using X-ray fluorescence (XRF). Powdered samples mixed with a binder were pressed into pellets. Empirical calibration was performed using standards of known elemental composition. Crust fragments, mounted on SEM stubs, were examined on a Supra 50 LEO-141 variable pressure scanning electron microscope (VPSEM) system.

#### 5. Results

##### 5.1 Megascopic description

Polished slabs of the hard upper crust samples showed a massive, brownish, finely crystalline material with abundant black spots

and well-developed desiccation cracks perpendicular to the mammillary surface (Figure 2D). Some specimens of this crust are vuggy and laminated. The lower crust is relatively thin and displays a dense network of desiccation cracks (Figure 2E).

##### 5.2 Microscopic description

###### 5.2.1 Dolomite

The light brown lower crust typically has an undulating sharp contact with the nodular calcretes (Figure 3A), whereas the hard, dark brown upper crust is thicker and has a diffused, corrugated contact (Figure 3B). The latter is extensively fractured and includes rhizolithic features, which consist mostly of root casts and moulds (Figure 3C). The light brownish crust commonly consists of euhedral to subhedral, moderately to poorly sorted dolomite grains floating in a micritic groundmass (Figure 3D). Dolomite grains vary in size between  $< 50 \mu\text{m}$  to  $400 \mu\text{m}$  and commonly occur as subrounded to subangular broken and corroded crystal fragments (Figure 3E). Some grains preserve rhombic shapes. The micritic groundmass is tinted light brown and commonly includes silt-sized haematitic grains. This crust is mostly micrite-supported; dolomite grains vary in abundance between 25% and 50% of the crust. The texture of this crust suggests a detrital origin.

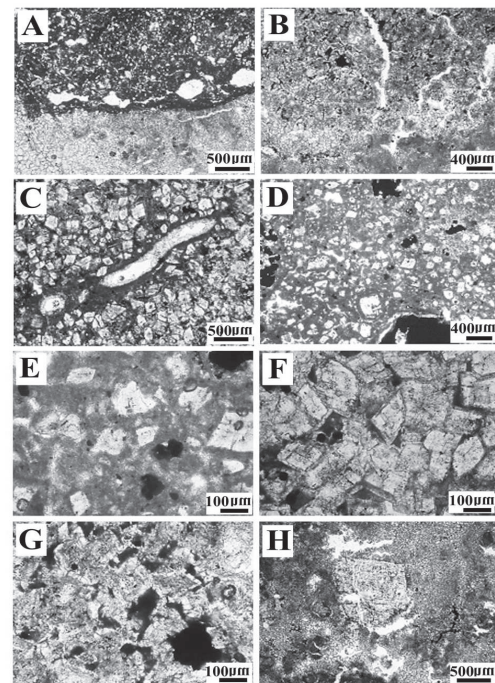


**Figure 3.** Microphotographs of the dolomitic crust. (A) Sharp contact between the crust (upper part) and the nodular calcretes (lower part); (B) a diffused contact; (C) root casts and moulds in the authigenic dolomitic crust; (D) detrital dolomite grains floating in a micritic groundmass; (E) subangular, corroded dolomite grains; (F) idiomatic mosaic of euhedral dolomite crystals; (G) mosaic of zoned dolomite with intercrystalline pore spaces are filled with brown-tinted micrite and iron oxides; (H) discrete coarsely crystalline euhedral dolomite in partially dolomitised calcrete.



The dark brown crust typically consists of an idiotopic mosaic of moderately sorted, euhedral dolomite crystals that reach a maximum size of 200  $\mu\text{m}$  (Figure 3F). Dolomite crystals are cloudy because of abundant inclusions, and some are zoned. The latter usually have a cloudy core and a thin, clear limpid zone several microns thick. The intercrystalline pore spaces are filled with tinted brown micrite and iron oxides (Figure 3G). Coarsely crystalline dolomite is also scattered within some of the pedogenic calcrete nodules. This dolomite occurs as cloudy euhedral crystals that vary in size from 100  $\mu\text{m}$  to 1 mm (Figure 3H). The texture of this crust indicates an authigenic origin

### 5.2.2 Dedolomitisation

Examination of stained thin sections revealed that most of both the detrital and authigenic dolomite crusts have been partially or completely dedolomitised. In the detrital dolomitic crust, partial dedolomitisation is commonly observed along crystal borders and cleavage planes (Figure 4A). The dolomite is partially or completely replaced by a mosaic of subhedral to anhedral calcite microspar (10–15  $\mu\text{m}$ ). The latter is partially dissolved, which has led to the occurrence of hollow dolomite rhombs (Figure 4B). Remnants of dolomite appear as cleavage fragments floating in the dedolomite mosaic. Some of these crusts appear as a mosaic of calcite microspar with ghosts of completely dedolomitised dolomite (Figure 4C). Ghosts are preserved by rinds of inclusion-rich microspar. It is suggested that this texture may have resulted from aggradational neomorphism of the micrite matrix that enclosed the detrital dolomite. Where inclusion-rich microspar rinds are lacking, there is complete disappearance of the original detrital dolomite, and the crust displays a clotted mosaic of poorly sorted microspar and sparry calcite (Figure 4D). This mosaic is enriched in iron oxides, which fill intercrystalline pores and are responsible for the brownish colouration of the crust. These iron oxides consist mostly of hematite, which occurs as agglomerations of euhedral six-sided crystals up to 100  $\mu\text{m}$  in size. The detrital dolomite in some of these crusts resisted dedolomitisation and appears as detrital dolomite floating in a groundmass of a mixture of clotted micrite and microspar. Some of this dolomite is surrounded by columnar calcite microspar to form corona-like structures (Figure 4E) and appears as calcrete with dolomite framework grains.

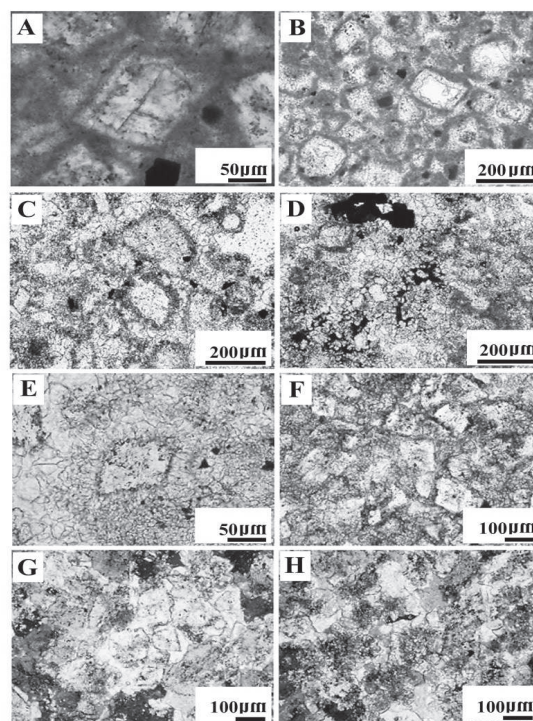


**Figure 4.** Microphotographs of dedolomite textures. (A) Partially dedolomitised detrital dolomite along the borders and cleavage planes, stained thin section; (B) mosaic of microsparry calcite replacing dolomite, with some dolomite grains partially dissolved; (C) ghosts of dolomite grains floating in a mosaic of calcite microspar; (D) completely dedolomitised detrital dolomitic crust displaying a clotted mosaic of poorly sorted microsparry and sparry calcite with abundant iron oxides; (E) detrital dolomite surrounded by a corona of columnar calcite microspar; (F) slightly dedolomitised dolomite rhombs floating in a mosaic of calcite microspar, stained thin section; (G) coarsely crystalline calcite crystal poikilotopically encasing several ghosts of completely dedolomitised pre-existing dolomite rhombs (crossed nicoles); (H) authigenic dolomitic crust, grumeleuse texture of completely dedolomitised dolomite (crossed nicoles).

Two textures were recognised in the dedolomitised authigenic dolomite crust. The first displays slightly dedolomitised dolomite rhombs floating in a calcitic microspar mosaic. Dedolomitisation is manifested as slight replacement of the edges of the dolomite rhombs and precipitation of calcite microspar between the dolomite rhombs. This texture resembles that of incipient calcretisation, where the precipitated microspars displace the host dolomite crystals. Altogether, it appears as incipiently calcretised dolomite (Figure 4F). The second texture results from complete dedolomitisation of the dolomitic crust. The dolomite mosaic has been replaced by a mosaic of anhedral,

coarse calcite crystals about 0.8 mm in size. Individual calcite crystals poikilotopically encase several ghosts of pre-existed dolomite rhombs (Figure 4G). These ghosts of dolomite rhombs are preserved as thin, dark rinds. In crusts characterised by inclusion-rich dolomite that lacks the aforementioned dark rinds, complete dedolomitisation results in a mosaic of sparry calcite with scattered islands of inclusions representing the pre-existing dolomite; the borders of this pre-existing dolomite can be seen as ghosts within the sparry calcite (Figure 4H). This appearance is similar to the "grumeleuse" texture described by Kenny (1992). The coarse dolomite crystals that are scattered within some of the pedogenic calcrete have also been dedolomitised. Each of these crystals has been replaced by a single calcite crystal that includes dense clusters of haematite arranged on its borders and cleavage planes.

SEM images have been captured to show both the detrital and authigenic types of the dolomite crust (Figure 5A and B). Both types are extensively dedolomitised (Figure 5C). These images also indicate partial dolomitisation of some calcrete nodules, manifested by the occurrence of euhedral dolomite rhombs about 60  $\mu\text{m}$  in size filling cavities and fractures (Figure 5D). Dolomites in the dedolomitised crusts display dissolution features, which consist mainly of grooves and holes oriented along the cleavage planes (Figure 5E). The cores of the zoned dolomites are preferentially dissolved (Figure 5F).

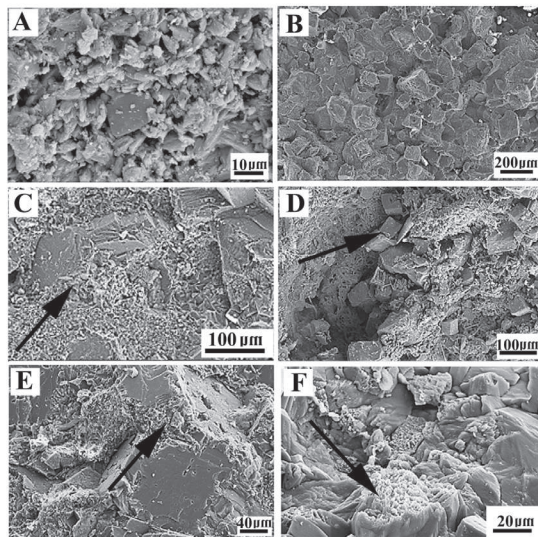


**Figure 5.** SEM images of the crust. (A) Detrital dolomite grain floating in a mosaic of microcrystalline calcite; (B) euhedral dolomite rhombs of the authigenic dolomitic crust; (C) arrow pointed at microsparry calcite (dedolomite); (D) authigenic dolomite fill of some cavities in calcrete; (E) partially dissolved and dedolomitised dolomite rhombs (arrow); (F) preferential dissolution of the cores of zoned dolomite (arrow).

### 5.3 Mineralogy and geochemistry

XRD analysis of the studied crusts revealed that they consist mostly of calcite and dolomite with traces of quartz (Table 1). The relative abundance of calcite reflects the extensive dedolomitisation of these dolomitic crusts. Significant variation was recognised in the mineralogical compositions of the detrital and authigenic dolomite crusts (Figure 6). The first is mostly calcitic; on average, calcite and dolomite constitute 91.11% and 7.44% of the samples, respectively. The abundance of calcite is attributed to the original micrite and the extensively calcitised (dedolomitised) detrital dolomite. The authigenic dolomitic crust is comparatively rich in dolomite, which reaches up to 40%, with an average of 28.33%.

The results of the geochemical analysis reflect the mineralogical composition of the crust (Table 1). The crust samples are composed mostly of CaO, which reflects the abundance of calcite. The average CaO contents of the authigenic and detrital dolomitic crusts are 44.94% to 49.68%, respectively, and the average MgO contents are 1.56% and 4.24%, respectively. These findings indicate that the higher abundance of calcite is at the expense of dolomite. Both types of crust are characterised by abundant Fe<sub>2</sub>O<sub>3</sub>, up to 4.88% in one sample in the authigenic dolomitic crust. Traces of Al<sub>2</sub>O<sub>3</sub>, SiO<sub>2</sub> and K<sub>2</sub>O may represent remnants of the terra rossa soil. The average Sr content ranges from 64 to 123 ppm, respectively, in the detrital and authigenic dedolomitised crusts.

**Table 1.** Concentrations of major oxides and Sr in the dolomitic crust.

Sample No.	Major oxides %											Sr (ppm)	LOI %	Mineralogy		
	CaO	MgO	Fe <sub>2</sub> O <sub>3</sub>	SiO <sub>2</sub>	Al <sub>2</sub> O <sub>3</sub>	K <sub>2</sub> O	Na <sub>2</sub> O	TiO <sub>2</sub>	MnO	SO <sub>3</sub>	P <sub>2</sub> O <sub>5</sub>			Dolomite	Calcite	Quartz
Authigenic dolomite crust																
1DD	42.28	5.49	1.33	5.46	2.74	0.84	0.56	0.12	0	0.06	0	160	41.01	37	63	0
2DD	41.68	6.24	0.52	2.03	0.96	0.33	1.34	0.07	0	0.06	0.02	170	46.56	40	59	1
3DD	44.78	4.04	1.63	3.16	1.38	0.49	1.62	0.09	0.02	0.06	0.00	100	42.54	25	73	2
4DD	47.22	3.03	1.55	2.44	1.02	0.26	1.64	0.11	0.00	0.03	0.00	110	42.51	20	79	1
5DD	46.09	3.18	1.17	2.46	1.10	0.37	1.54	0.08	0.01	0.03	0.00	98	43.76	30	68	2
6DD	47.61	3.44	1.31	1.85	0.80	0.32	0.73	0.05	0.00	0.05	0.02	100	43.72	18	80	2
Average	44.94	4.24	1.25	2.90	1.33	0.44	1.24	0.09	0.01	0.05	0.01	123	43.35	28.33	70.00	1.33
Detrital dolomite crust																
1DC	52.82	0.62	0.61	2.38	0.86	0.01	1.01	0	0	0.03	0.01	43	41.42	0	100	0
2DC	47.3	2.52	1.55	2.35	0.72	0.08	2.94	0.05	0.01	0.01	0	69	42.18	15	83	2
3DC	47.96	2.1	1.01	4.72	1.52	0.11	1.32	0.06	0	0.09	0.01	62	40.89	13	86	1
4DC	52.68	0.63	0.17	3.16	1.07	0.01	0.88	0.02	0	0.03	0	58	41.23	0	97	3
5DC	48.48	1.54	4.88	1.31	0.48	0.1	2.04	0.05	0.08	0.04	0.01	61	39.05	5	94	1
6DC	53.04	0.89	0.28	2.32	0.83	0.07	0.96	0.04	0	0.04	0.02	58	41.37	5	93	2
7DC	51.05	1.25	1.5	2.6	1.08	0.37	1.31	0.08	0	0.04	0	87	40.53	3	95	2
8DC	44.92	2.48	3.56	4.39	2.00	0.75	1.01	0.12	0.00	0.05	0.02	70	40.52	12	88	0
9DC	48.87	2.01	2.97	3.85	1.78	0.62	0.41	0.12	0.00	0.04	0.02	65	39.21	14	84	2
Average	49.68	1.56	1.84	3.01	1.15	0.24	1.32	0.06	0.01	0.04	0.01	64	40.71	7.44	91.11	1.44

## 6. Discussion

The field occurrence, petrography and geochemistry of the studied crust are interpreted to reveal a complex paragenesis. Field observations suggests that the material of this crust was derived from outside its location, mostly from the nearby weathered dolomitic sequence of Triassic and Jurassic dolostone. Vandeginste & John (2012) reported that the Jurassic dolostones exposed in the Al-Jabal Al-Akhdar region near the study area have been weathered significantly during the Pleistocene and Holocene to form a blanket of detrital dolomite, dedolomite and geothite. This weathered mantle was susceptible to transportation by surface runoff during the early and middle Holocene pluvial periods (Clemens *et al.*, 1996; Burns *et al.*, 2001; Neff *et al.*, 2001).

It is suggested that this surface runoff was enriched considerably in Ca and Mg and loaded with detrital dolomite grains. Such surface runoff with its load has been infiltrated through the fractured pedogenic calcrete horizon in the study area. Because of the southward shift of the monsoon rainfall belt, this area was subjected to a relatively dry period in the late Holocene, during which the detrital dolomite-bearing solution was subjected to evaporation and became saturated with respect to calcite. Eventually, calcite precipitated to form the light brown detrital dolomitic crust. The precipitation of

calcite depleted dissolved Ca and increased the Mg/Ca ratio, and the remaining solution became saturated with respect to dolomite. Consequently, dolomite has been precipitated from this solution under evaporation condition during dry periods (Carlisle, 1983; Arakel, 1986; Jacobson *et al.*, 1988).

The texture and fabrics of this dolomite crust suggest an authigenic origin. However, the trapped micrite within the intercrystalline pore spaces in the well-developed dolomite rhombs may represent sediments suspended in the infiltrated surface runoff. The occurrence of the scattered dolomite rhombs within the calcrete nodules in close contact with this crust as well as the lack of direct or indirect indications of precursor calcite suggest that this dolomite has been precipitated from pore solutions saturated with respect to dolomite (Khalaf, 1990). The euhedral form of this dolomite may provide an additional evidence of its authigenic origin.

The dolomitic crusts were then subjected to extensive dedolomitisation as a result of their flushing by highly oxidised meteoric water with a high Ca/Mg ratio. The occurrence of dedolomite as a mosaic of microspar around the detrital dolomite grains and within intracrystalline dissolution cavities may suggest a two-step process: dissolution of dolomite followed by precipitation of calcite



(dedolomite) (Warrak, 1974; Kenny, 1992). The possibility of detrital dedolomite transportation from the source should not be ignored. Conversely, the texture and fabric of the dedolomitised authigenic dolomite crust may suggest that the dedolomitisation processes occurred simultaneously and relatively slowly (Evamy, 1967; Al-Hashimi & Hemingway, 1973; Back *et al.*, 1983; Khalaf & Abdal, 1993). The relative abundance of dolomite within the dedolomitised authigenic dolomitic crust may suggest that it is more resistant to dedolomitisation compared with that in the dedolomitised detrital dolomitic crust.

The above discussion suggests that the dedolomitised crust was formed by deposition of the detrital dolomite crust followed by precipitation of the authigenic dolomite crust during dry periods. These steps were followed by dedolomitisation during wet periods. Table (2)

demonstrates the paragenetic history of the formation of the studied dedolomitised dolomitic crust. The availability of source rock and the intermittent wet and dry prevailing climatic conditions have played significant roles in the development of this crust. The occurrence of the dedolomite crust on pedogenic nodular calcretes and the partial dolomitisation and dedolomitisation of these calcretes suggest that the formation of the crust postdates that of the calcretes, which indicates that this crust has developed during the present semi-arid prevailing climate with intermittent wet and dry periods (Mann & Horwitz, 1979; Carlisle, 1983). It should also be noted that by the advent of aridity, these crusts could be subjected to erosion and therefore provide source of aeolian detrital dolomite and dedolomite (Khalaf *et al.*, 1994).

**Table 2.** The paragenetic history of the dedolomitized dolomitic crust

Climate	Processes	Chronological sequence						Products
		Stage I	Stage II	Stage III	Stage IV	Stage V	Stage VI	
Mid- Holocene Pluvial period	Localized Dissolution of the calcareous bedrocks and erosion and transportation of terra rossa soil	█						Formation of localized cavities filled with terra rossa soil
Recent semi-arid period	Precipitation of biogenic calcite from meteoric water supersaturated with respect to calcite		█					Development of pedogenic calcrete within and displacing terra rossa cavity fill soil
Present Intermittent wet and dry periods	Flowing of rain water loaded with detrital dolomite grains on the cavity fill calcrete along fractures			█				Calcrete covered with slurry of detrital dolomite in solution rich in Ca and Mg
	Evaporation and precipitation of microcrystalline calcite				█			Formation of the detrital dolomite crust cemented by calcite
	Further evaporation					█		Formation of authigenic dolomite crust
Present wet period	Flushing the dolomitic crust by highly oxidized meteoric water with high Ca/Mg ratio.						█	Dedolomitization of the detrital and authigenic dolomite crust

**7. Conclusions**

These pedogenic calcretes within karstic terra rossa soil are crusted with rusty dedolomite. Field observations and petrographic examinations indicate that this crust consists of two lithotypes: detrital and authigenic dedolomitised dolomite. The first type developed from the flow of carbonate-rich oxidised meteoric water loaded with detrital dolomite grains through the fractured pedogenic nodular calcrete horizon during wet periods. Detrital dolomite grains may have been derived from the weathered dolostone formations

exposed at higher elevations. The detrital dolomite crust developed due to evaporation during arid periods. These processes led to an increase of Mg/Ca ratio in the remaining water, and eventually, authigenic dolomite crust precipitated during dry periods. This crust was flushed with oxidised meteoric water during rainy seasons, which resulted in its dedolomitisation. It is concluded that this crust has been developed during the present semi-arid prevailing climate characterised by intermittent wet and dry periods.

## 8. Acknowledgements

The authors appreciate the support provided by the Electron Microscopy Unit (EMU) of Kuwait University. This study was partially supported by SAF Grant Number GS0105/, GS0301/. Thanks are extended to Mr. Al-Tabei for help in conducting the XRD analysis and to Mr. Sabir for use of the XRF laboratories of the Faculty of Science, Kuwait University. Special thanks are also extended to Mr. Nabil Basily and Mr. Yousef Abdullah for their help with laboratory work and thin section preparations. Help provided by Mr. Hisham during field work is greatly appreciated.

## References

- Al-Busaidi, M. (2012).** The struggle between nature and development: Linking local knowledge with sustainable natural resources management in Al-Jabal Al-Akhdar Region, Oman. PhD thesis, University of Glasgow, School of Geographical and Earth Sciences. P 433.
- Al-Hashimi, W.S. & Hemingway, J. E. (1973).** Recent dedolomitization and the origin of the rusty crusts of Northumberland. *Journal of Sedimentary Petrology*, **43**:82-91.
- Arakel, A.V. (1986).** Evolution of calcrete in palaeodrainages of the lake Napper Area, central Australia. *Palaeogeography Palaeoclimatology Paleocology*, **54**:283-303.
- Back, W., Hanshaw, B.B., Plummer, L.N., Rahn, P.H., Rightmire, C.T. et al. (1983).** Process and rate of dedolomitization: Mass transfer and <sup>14</sup>C dating in a regional carbonate aquifer. *Geol. Soc. Amer. Bull.*, **94**:1415-1429.
- Baud, A. & Richoz, S. (2013).** Permian–Triassic Transition and the Saiq/Mahil Boundary in the Oman Mountains: Proposed correction for lithostratigraphic nomenclature. *GeoArabia*, **18**:87-98.
- Budai, J.M., Lohmann, K.C. & Owen, R.M. (1984).** Burial dedolomite in the Mississippian Madison Limestone, Wyoming and Utah thrust belt. *Journal of Sedimentary Petrology*, **54**: 276-288.
- Burns, S.J., Fleitmann, D., Mudelsee, M., Neff, U., Matter, A. et al. (2001).** Speleothem evidence from Oman for continental Pluvial events during Interglacial 1 Periods. *Geology*, **29**(7):623-626.
- Cantrell, D.L., Al-Khamash, A. & Jenden, P.D. (2007).** Characterization and significance of dedolomite in Wadi Nisah, central Saudi Arabia. *GeoArabia*, **12** (3):15–30.
- Carlisle, D. (1983).** Concentration of uranium and vanadium in calcretes and gypcretes. In: *Residual Deposits* (Ed. by R. C. L. Wilson). Geological Society of London, Special Publication, **11**:185-195.
- Carpenter, A.B., Trout, M.L. & Pickett, E.E. (1974).** Preliminary report on the origin and chemical evolution of lead- and zinc-rich oil field brines in central Mississippi. *Economic Geology*, **69**:1191-1206.
- Chafetz, H.S. (1972).** Surface diagenesis of limestone. *Journal of Sedimentary Petrology*, **42**: 325-329.
- Chilingar, G.V. (1956).** Dedolomitization: A review. *American Association of Petroleum Geologists Bulletin*, **40**: 762-778.
- Clemens, S.C., Murray, D.W. & Prell, W.L. (1996).** Nonstationary phase of the Plio-Pleistocene Asian monsoon. *Science*, **274**:943-948.
- Coniglio, M. (2003).** Dedolomitization. In: *Encyclopedia of Earth Science*. Part 4: Sedimentology, pp 300-303.
- De Groot, K. (1967).** Experimental dedolomitization. *Journal of Sedimentary Petrology*, **37**: 1216-1220.
- Dickson, J.A.D. (1966).** Carbonate identification and genesis as revealed by staining. *Journal of Sedimentary Petrology*, **36**:491-505.
- Dixon, J.C. (2010).** Origin of calcrete and dolocrete in the carbonate mantle of St Vincent Basin, southern South Australia. *Cadernos Lab. Xeoloxico de Laxe Coruna*, **35**:109-122.
- Escorcía, L.C., Gomez-Rivas, E., Daniele, L. & Corbella, M. (2013).** Dedolomitization and reservoir quality: insights from reactive transport modelling. *Geofluids*, **13**: 221–231.
- Evamy B.D. (1967).** Dedolomitization and the development of rhombohedral pores in limestones. *Journal of Sedimentary Petrology*, **37**:1204-1215
- Goldberg, M. (1967).** Supratidal dolomitization and dedolomitization in Jurassic rocks of Hamakhtesh Haqatan, Israel. *Journal of Sedimentary Petrology*, **37**: 760-773.
- Holail H., Lohmann K.C. & Sanderson, I. (1988).** Dolomitization and dedolomitization of Upper Cretaceous carbonates; Babariya Oasis, Egypt, In: V. Shukla and P.A. Baker (Editors), *Sedimentology and Geochemistry of Dolostones*. Soc. Eeon. Paleontol. Mineral. Special Publication, **43**:191-207.
- Hutton, J.T. & Dixon, J.C. (1981).** The chemistry and mineralogy of some South Australian calcretes and associated soft carbonates and their dolomitization. *Geological Society of Australia*, **28**:71-79.
- Jacobson, G., Arakel, A.V. & Yijian, Ch. (1988).** The central Australian groundwater discharge zone: Evolution of associated calcrete and gypcrete deposits. *Australian Journal of Earth Science*, **35**:549-565.



- James, N.P., Bone, Y.& Kyser, T.K.(1993).** Shallow burial dolomitization and dedolomitization of mid-Cenozoic, cool-water, calcitic, deep-shelf limestones, southern Australia. *Journal of Sedimentary Petrology*, **63**:528-538.
- Jones, B., Pleydell, S.M., Ng, K.C.& Longstaffe, F.J.(1989).** Formation of poikilotopic calcite-dolomite fabrics in the Oligocene-Miocene Bluff formation of Grand Cayman, British West Indies. *Bulletin of Canadian Petroleum Geology*, **37**:255-265.
- Katz, A. (1968).** Calcian dolomites and dedolomitization. *Nature*, **217**:439-440
- Kenny, R. (1992).** Origin of disconformity dedolomite in the Martin Formation (Late Devonian, northern Arizona). *Sedimentary Geology*, **78**:137-146.
- Khalaf, F.I.& Abdal, M.S. (1993).** Dedolomitization of dolomite deposits in Kuwait, Arabian Gulf. *Geologische Rundschau*, **82**:741-749
- Khalaf, F.I.& Al-Zamel, A. (2016).** Petrography, micromorphology and genesis of Holocene pedogenic calcrete in Al-Jabal Al-Akhdar, Sultanate of Oman. *Catena*, **147**: 496-510.
- Khalaf, F.I., Al-Ajmi, D.& Al-Dousari, A.(1994).** Detrital palygorskite in recent terrestrial and marine sediments of Kuwait. *Egyptian Journal of Geology*, **38** (2): 537-554.
- Khalaf, F.I. (1990).** Occurrence of phreatic dolomite within Tertiary clastic deposits of Kuwait. *Arabian Gulf. Sedimentary Geology*, **68**: 223-239.
- Kharaka, Y.K., Callender, E.& Wallace, R.H. (1977).** Geochemistry of geopressed geothermal waters from the Frio Clay in the Gulf Coast region of Texas. *Geology*, **5**: 241-244.
- Koehrer, B., Zeller, M., Aigner, T., Poepplreiter, M., Milroy, P., Forke, H.& Al-Kindi, S. (2010).** Facies and stratigraphic framework of a Khuff outcrop equivalent: Saiq and Mahil formations, Al Jabal al-Akhdar, Sultanate of Oman. *GeoArabia*, **15**: 91-156.
- Land, L.S.& Prezbindowski, D.R. (1981).** The origin and evolution of saline formation water, Lower Cretaceous carbonates, south-central Texas, U.S.A. *Journal of Hydrology*, **54**: 51-74.
- Mann, A.W.& Horwitz, R.C. (1979).** Groundwater calcrete deposits in Australia: some observations from Western Australia. *Journal of the Geological Society of Australia*, **26**:293-303.
- Nader, F.H., Swennen, R.& Keppens, E. (2008).** Calcitization/dedolomitization of Jurassic dolostones (Lebanon): results from petrographic and sequential geochemical analyses. *Sedimentology*, **55**:1467-1485.
- Neff, U., Bums, S.G., Mangini, A., Mudelsee, M., Fleitmann, D.&Matter, A. (2001).** Strong coherence between solar variability and the monsoon in Oman between 9 and 6 kyr ago. *Nature*, **411**: 290-293.
- Netterberg, F. (1980). *Geology of Southern African calcretes: 1. Terminology, description, macrofeatures, and classification.* *South African Journal of Geology*, **83**:255-283.
- Phillips, S.E.& Milnes, A.R. (1988). The Pleistocene terrestrial carbonate mantle on the southeastern margin of the St. Vincent Basin, South Australia. *Australian Journal of Earth Science*, **35**:463-481.
- Rameil, N. (2008). Early diagenetic dolomitization and dedolomitization of Late Jurassic and earliest Cretaceous platform carbonates: A case study from the Jura Mountains (NW Switzerland, E France). *Sedimentary Geology*, **212**(1-4): 70- 85.
- Saddiqi, O., Michard, A., Goffe, B., Poupeau, G.& Oberhansli, R. (2006). Fission-track thermochronology of the Oman Mountains continental windows, and current problems of tectonic interpretation: *Societe Geologique de France Bulletin*, **177**: 127-134.
- Stoessell, R.K., Klimentidis, R.E.& Prezbindowski, D.R.(1987). Dedolomitization in Na-Ca-Cl brines from 100° to 200°C at 300 bars. *Geochimica et Cosmochimica Acta*, **51**: 847-855.
- Theriault, F.& Hutcheon, L. (1987). Dolomitization and calcitization of the Devonian Grosmont Formation, Northern Alberta. *Journal of Sedimentary Petrology*, **6**: 955-966.
- Vandeginste, V.& John, C.M. (2012). Influence of climate and dolomite composition on dedolomitization: insights from a multi-proxy study in the Central Oman Mountains. *Journal of Sedimentary Research*, **82**: 177-195.
- Von Morlot, A. (1847). *Veber Dolomit und seine Kunstliche Darstellung aus Kalkstein: Naturwissenschaftliche Abhandlungen, gesammelt und durch Subscription lursg: Von Wilhelm Haidinger*, **1**:305-315.
- Warrak, M.(1974). The petrology and origin of dedolomitized veined or brecciated carbonated rocks, the cornieules, in the Frejus region, French Alps. *Journal of Geological Society*, **130**: 229-247.
- Watts, N.L. (1980). Quaternary pedogenic calcretes from the Kalahari (Southern Africa): Mineralogy, genesis and diagenesis. *Sedimentology*, **27**:661-686.

Submitted: 11/02/2017

Revised : 24/04/2017

Accepted : 30/04/2017

## تواجد قشرة من الديدولوميت الحديث على رواسب الكالكريت بمنطقة الجبل الأخضر – شمال سلطنة عمان

فكرى خلف\* ، عبد الله الزامل

قسم علوم الأرض والبيئة، كلية العلوم، جامعة الكويت

\*Fikry—khalaf@hotmail.com

### خلاصة

تتواجد قشرة من الديدولوميت على شقوق برواسب الكالكريت في التربة الحمراء داخل تجاويف فيتوكارستية ضحلة في الصخور الجيرية المكشوفة في منطقة الجبل الأخضر بسلطنة عمان. تم التعرف على نوعين من هذه القشرة الصخرية: (أ) ديدولوميتيزيد دولوميت منقول و (ب) و ديدولوميتيزيد دولوميت ترسيبي. النوع الأول يتسم بلون بني فاتح ويتلامس مع الكالكريت العقدى على سطح حاد و موج ويتكون من حبيبات من الدولوميت غير منتظمة الشكل و متنوعة الاحجام تسبح في نسيج من بلورات الكالسيت دقيقة الحجم. أما النوع الثاني أكثر سمكا نسيبا، ولونه بني داكن، ويتألف من فسيفساء من بلورات الدولوميت منتظمة الشكل و الحجم و يصل حجمها إلى 200 ميكرون. وأظهر الفحص المجهرى لشرائح ميكروسكوبية مصبوغة أن معدن الدولوميت بهذه القشور قد استبدلت جزئيا أو كلياً ب ديدولوميت. و قد بينت تحاليل هذه القشور بواسطة أشعة الحيود الطيفي (XRD) أن كلا النوعين من القشور تتكون في الغالب من الكالسيت والدولوميت مع آثار الكوارتز، حيث تعكس وفرة الكالسيت الى تحوله الى ديدولوميت. ويعكس التركيب الكيميائي لهذه القشور تكوينها المعدنى. وقد ناقش البحث التغيرات المعدنية التى طرأت على هذه القشور و تتابع حدوثها. ويعزى تكون هذه القشور الى توافر صخور المصدر الدولوميتي وطبيعة مناخ المنطقة الحالى شبه الجاف و الذى يتميز بفترات متعاقبة من الرطوبة والجفاف. و يعرض هذا البحث طريقة فريدة للتغيرات التى تحدث للدولوميت المصاحب لرواسب الكالكريت العقدى بالتربة الحمراء.